AADE-19-NTCE-080

How Does Buckling Impact Drilling & Completion Performance in Unconventional Wells?

Stephane Menand, Mahmoud Farrag, DrillScan

Abstract

The intent of this paper is to better educate the industry on the importance of advanced buckling evaluation in achieving well objectives and to highlight some of the limitations in the way the industry discusses and uses the buckling limits in their current form.

The drilling industry experiences buckling frequently especially in unconventional wells, however the basic mechanics of how it is initiated and propagated and the consequences on tubulars are sometimes misunderstood or oversimplified. This can lead to an inability to reach total depth with a completion string, a failure along the drilling string or most commonly, a loss of sliding ability towards the end of the lateral. By exploring typical buckling in unconventional type wells, recommendations to avoid some of these common and costly lock-up and failures are made.

By examining a detailed buckling model with advanced contact point management and comparing it with the industry standard method, some of the differences between the two are highlighted. For example, the effects of friction, rotation and surveys spacing are important in buckling evaluation but are ignored in most published methods. Case studies in which simple buckling analysis early on lead to failure and lock-up in the well construction process are presented as learning opportunities.

Comparing the advanced buckling model with the current industry standard method and exploring a variety of buckling scenarios in actual unconventional wells, advances the knowledge of the industry's quantification and evaluation of buckling.

Introduction

Buckling occurs when the compressive load in a tubular exceeds a critical value, beyond which the tubular is no longer stable and deforms into a sinusoidal or helical shape (constrained buckling).

It is worth noting that these two special shapes are a particular case for a given situation. Depending on the hole geometry, the shape of the buckled drill strings may take different forms (Menand *et al*. 2008, 2009, 2011, 2013). The sinusoidal buckling (first mode of buckling) corresponds to a tube that snaps into a sinusoidal shape and is sometimes called lateral buckling, snaking, or 2D buckling. This form of buckling is not very harmful in terms of additional stress on the string but might trigger lateral vibrations when rotating the pipe (lateral oscillation).

The helical buckling (second mode of buckling) corresponds to a tube that snaps into a helical shape (spiral shape). Lubinski started the first work dedicated to the buckling behavior of pipes in oilwell operation (Lubinski 1950; Lubinski *et al.* 1961). Since then, many theoretical works and/or experimental studies (see complete Reference list) have been developed to better understand and model the buckling phenomenon and to take into account the effects caused by wellbore geometry, dogleg severity, torque/torsion, tool joints, friction, and rotation. The standard equation used to predict the occurrence of helical buckling in a perfect straight/deviated wellbore is

$$F_{hel} = k \sqrt{\frac{EI\omega \ sin(Inc)}{r}} \qquad \text{(Eq. 1)}$$

The k number varies from 2.83 to 5.65, depending on the author and on the different assumptions made. In conducting laboratory experiments and numerical analyses in a perfect horizontal well without rotation, Menand *et al.* (2006) and Tikhonov *et al.*(2006) found similar results on the relationship between k and the deformed shape of the drill pipe: The k number close to 2.83 predicts the onset of the first helix, and the k number close to 5.65 predicts the full helical drill string deformation in a perfect wellbore geometry (without rotation).

After deriving equations for straight wells (vertical, inclined, horizontal), some authors extended some existing equations for a mono-curved borehole or developed new theories for tubular strings in curved wells (Schuh 1991; Kyllingstad 1995). It's worth mentioning that these simple equations can only be derived on some idealized cases where mathematics are simple enough to find an analytical solution.

However, recent studies (Menand *et al*) have shown that the conventional sinusoidal and helical-buckling criteria are accurate only in a perfect wellbore geometry because wellbore tortuosity and doglegs play a great role in the buckling phenomenon. An example is illustrated in Fig. 1 by use of

numerical simulations, which shows that sinusoidal, helical or any shape of buckling might take place anywhere depending mainly on tortuosity and/or dog leg, friction, hole size and contact points. Having a simple equation that can catch the full buckling situation is unfortunately impossible.

Buckling in Unconventional Plays

Compression on the string is maximal when tripping in, running casing/liner, or drilling in sliding mode with a given weight on bit (WOB). Buckling may also occur when drilling with a rotary assembly with a large WOB as the critical helical-buckling load for a rotating pipe may be approximately 50% less than that obtained for a non-rotating pipe (Menand *et al.* 2008, 2009). This rotation effect can be mainly attributed to the friction phenomenon that makes the pipes roll more easily on the wall of the borehole and eases the onset of buckling and/or instability. Given the same compression, it is thus easier to buckle a rotating pipe than a non-rotating pipe. The helical-buckling load is generally the load used in drill string or casing design to define the limit upon which the tubular might be fully buckled with the risk of getting stuck or with the risk of large bending stresses that may lead to failure. During the well-planning process, if the compression in the drill string exceeds the critical helical-buckling load (see Eq. 1), drilling engineers usually modify the drill string design until this buckling does not occur. Fig. 2 shows an example of a typical compressive-load analysis when drilling a horizontal wellbore. This result has raised questions for drilling engineers regarding whether they should modify the design and/or try to reduce the coefficient of friction with the help of lubricants for example. It is widely recognized that sinusoidal buckling is not harmful to tubular (additional contact force and stress is limited), but helical buckling is generally perceived as a dangerous situation. Many people have suspected that the standard buckling criteria may be too conservative. Indeed, some previous studies (Newman *et al.* 1989) have shown that it is possible to safely push tubular into a highly deviated hole while exceeding the critical buckling load. A great number of field case studies have also reported that compressive loads greater than the helical-buckling load could be used to drill highly deviated wells. Results from previous studies (Menand *et al.* 2011; Menand 2012, 2013) have also suggested that helical buckling should not be systematically interpreted as a phenomenon that prohibits drilling or running-in-hole operations. It is also known that axial-force transfer usually remains good even though the pipe is helically buckled. However, most torque-and drag models lack the capability of the post-buckling calculations to model buckled strings (Mason and Chen 2007). The model utilized in this paper has post-buckling capabilities, meaning that pipe deflection, contact force, and stress is calculated once the pipe is buckled, leading to an increase of torque and drag.

Alternatively, Menand *et al.* (2011) has proposed a new Buckling Severity Index (BSI) that focuses more on the level of bending stress rather than the type and shape of buckling (sinusoidal or helical). This index ranges from 1 for a safe buckling condition to 4 for severe buckling, to quantify the risk of lockup or possible failure because of buckling. This index is based on the calculation and evaluation of three quantities: bending stress, contact side force, and von Mises stress, that can be evaluated with a conventional torque-and-drag calculation with stiff-string capability. This index enables to better quantify the severity of buckling as exceeding buckling can be safe (Menand *et al* 2013).

Unconventional shale plays are generally characterized by three main sections: vertical, curve and lateral, that present 3 different risks associated with buckling. Fig. 1 and 2 show the typical tension/compression plot and buckling situation when drilling in sliding mode with a steerable mud motor. The helical buckling load is generally exceeded along the vertical section (0-8,500ft) as shown in Fig. 2, and confirmed by the post-buckling model that shows the helical shape. However, the bending stress and contact forces are relatively low and do not influence weight transfer or fatigue in the vertical section. Past the kick-off point to start building the curve, one notices that the buckling severity index reaches the level 4, meaning that the bending stress and contact forces are high and generate a lot of drag forces and possible fatigue in case of rotation. The slide-rotate pattern created by a steerable mud motor can also make the situation worse as local dog legs can generate locally high contact or stress on the string (see Fig. 2, where one sees the effect of a high local dog leg along the curve). The heel of the lateral section is generally the section where compression can be very high, making the landing quite critical. Indeed, simulations shows that landing smoothly without exceeding the landing inclination is critical to avoid additional drag before drilling the lateral.

In rotary mode, buckling can happen along the lateral section with high WOB, especially if hole over gage is present (wash out, hole instability, high bend mud motor, etc…). Fig 1 shows a simulation where a caliper log was utilized to simulate the helical buckling along the lateral section. A higher hole over gage will increase the clearance r (see Eq. 1) and consequently reduce the critical buckling load Fc. In other words, it's easier to buckle a pipe in a larger borehole. Interestingly one notices that once the hole size is in gage, the buckling disappears (see Fig. 1 the section closer to the bit).

Case Study

Introduction

The case study presented in the next paragraph consists in analyzing 3 different steerable mud motor BHAs (exact same characteristics but different bend angle) to drill the same well shown in Fig. 3. The well is characteristic of shale wells with a 9 5/8in. casing shoe set high in the vertical section, around 4,000ft. A curve with planned doglegs around 10deg/100ft is landed in the shale with a 6,000ft lateral following it.

Table 1 shows the characteristics of the BHA, consisting of an 8 ½ in. PDC bit and a steerable mud motor assembly with a bend angle that has been varied from 1.5deg. to 2.2deg. The different bend angle will convert into a different steering program as obviously the BHA with the highest bend angle will

produce the highest build rate in sliding mode with a tool face up. For this application, one has calculated with a BHA model (Studer *et al*), that the BHA#3 will produce a build rate of about 16.5deg./100ft in sliding mode (TFO=0 deg.) and 0.0deg/100ft in rotary mode (see Fig. 4) with a given WOB. The BHA#2 build rate in sliding mode is about 12.0deg./100ft and 2.0deg./100ft in rotary mode. As for the BHA#1, one has assumed 100% of sliding along the curve with an average build rate of 10deg./100ft. The slide-rotate pattern is typical of steerable mud motors drilling the curve in unconventional play. Fig. 5 shows an example of an actual tortuosity modeled and measured with continuous inclination sensor (Menand *et al*). This example shows that the average build rate along the curve is about 6deg./100ft (standard surveys) but locally higher (16.5deg./100ft) in sliding mode. As we will see later in the paper, this slide-rotate pattern will affect the buckling behavior, not only along the curve but also along the lateral as a lot of friction/drag can be generated in these high local dog legs.

Also, one has assumed in the present application that the 3 BHAs with different bend angles will generate some hole overgage in rotating mode. It has been assumed in the following that the hole overgage was ¼ in. for the BHA#1 (1.5deg. bend), ½ in. for the BHA#2 (2.2deg. bend) and ¾ in. for the BHA#3. As discussed previously, hole over gage, wash-out can facilitate the onset of buckling as the gap between the tubular and the borehole is higher. Along the lateral section, one has assumed about 5, 10 and 15% of sliding (footage) for BHA#1, BHA#2 and BHA#3 respectively, and still assuming the same hole overgage in rotary mode.

In the next section, we study the buckling behavior of the drilling assembly and completion in the same well trajectory but characterized by 3 different levels of tortuosity (due to different BHAs and steering program) and hole overgage as discussed above.

Drilling Operations

Being able to drill and steer the well along the long lateral section of these unconventional wells can be very challenging, because of high torque, drag and buckling. The weight transfer in sliding mode can be very poor as high friction and buckling take place at many positions, especially along the curve where high compression and contact forces are observed.

Fig 2 shows the simulated tension/compression and side force along the drill string while drilling in sliding and rotary mode at target depth for the BHA#1 (1.5 deg. bend). First, one notices that the standard helical buckling load (Eq. 1) is largely exceeded when drilling in sliding mode along the vertical and curve section. As discussed previously, even though the helical buckling is observed in the vertical section, the bending stresses and contact forces are not so important. However, the Buckling Severity Index (BSI) reaches the level 4 in the curve indicating strong side forces and high bending stress as can be seen also in Fig. 6. Contacts on the pipe body are even observed due to the high local dog leg severity combined with high compression. One considers that a BSI equal to or greater than 3 requires particular attention and monitoring. The curve is a short section to drill but with high drag forces, meaning that drilling a smooth curve might help minimize the friction for the entire well.

Fig 7 shows a comparison between the 3 different BHAs (thus 3 different slide-rotate patterns) while sliding at target depth with the same 10klbs WOB. It's interesting to notice that there is about 40klbs tension difference at surface between the trajectories drilled by BHA#1 (smooth curve – 10deg/100ft curve) and by BHA#3 (slide-rotate pattern with local dog leg at 16.5deg./100ft). In other words, one can say that the slide-rotate pattern can generate about 40klbs more drag than a smooth (perfect) curve. This observation is also true when running a casing string or a completion as high friction can be generated in the curve. As buckling is a highly non-linear problem, a small change in the trajectory or the coefficient of friction can affect significantly the results. One recommends generally to run all simulations with several coefficients of friction as high as 0.4 or even 0.5 to anticipate any potential problems such as lock-up.

Fig. 8 shows the hook load and BSI while sliding with 10klbs WOB at several bit depths (BHA#1). This plot indicates that sliding can be difficult starting at about 12,500ft where the BSI reaches the level 4 (high contact forces). The BSI reported here corresponds to the maximum value along the string at a given bit depth. Having a surface oscillation system that rocks the pipe alternatively to the right and to the left can help overcome these limitations in sliding mode as the friction is transferred to the rotational movement, reducing significantly the compression along the string.

Completion

Running casing or completion at target depth is still a challenge in horizontal wells, especially with the presence of tortuosity or hole overgage. Special techniques such as floatation, rotation is now required to ease the run-in hole operations as drag in a major concern. The subject well presented in this paper is completed with a 5 ½ in. casing string (17ppf linear weight) with partial floatation of the string. The torque & drag & buckling model utilized in this analysis enables to model properly the behavior of the casing (filled with fluid, or air) in a 3D borehole and tortuosity, with optional rigid or flexible centralizers, fracturing sleeves, packers. The sensitivity analysis conducted in this paragraph consists in varying the length of floated casing string to see its effect on drag and buckling. Typically, the vertical casing section is filled with fluid (to provide weight) while the lateral section is floated, reducing the buoyant weight of the string, and thus reducing the drag force and compression (see Fig. 9) In the following, we'll see the effect of the slide-rotate pattern and floatation on buckling.

Four casing strings are studied: one with no floatation and 3 casing strings where the float length (starting from the casing shoe) is 2,500ft, 5,300ft and 6,600ft. Fig. 10 shows the 3D visualization of the casing string inside the curves drilled by BHA#1 (smooth curve – 10deg./100ft curve) and by BHA#3 (slide-rotate pattern with local dog leg at 16.5deg./100ft). The 2 simulations correspond to a run-in hole operation at target

depth without the use of floatation. As for the drilling assembly, the additional stress and contact force are significant in the curve drilled by BHA#3, especially through the high local dog leg (16.5deg./100ft), creating an additional drag of about 20klbs for the entire casing string.

Fig. 11 shows now the simulations of 2 casing string running in the hole at target depth in the trajectory drilled by BHA#3 (slide-rotate pattern with local dog leg at 16.5deg./100ft), with or without floatation. One notices clearly that the floatation enables to have a greater hook load at surface compared to the case without floatation (100klbs difference at surface). Also, as previously discussed the bending stress on the floated casing is significantly reduced, enabling to keep the integrity of the casing within safe limit.

Fig. 12 shows the same simulation with the buckling severity index. It's interesting to notice that the floated casing does not reduce the bending stress along the curve (strongly linked to the curvature of the borehole) but reduces only the level of contact forces as can be seen in Fig. 13. Also, one observes that the helical buckling is less pronounced in the vertical section when the casing string is floated (the compression is far less than the casing string with no floatation), even though side force and bending stress are within acceptable range.

Fig. 14 shows the hook load while running in the hole 4 different options for the casing: no floatation, 2,500ft, 5,300ft and 6,600ft of floatation. Getting the casing to target depth could be compromised in case of higher friction factor or high tortuosity without the use of floatation. On the contrary floating the casing enables to have a higher safety margin to be sure to reach target depth.

Conclusions

Drilling and running completion in unconventional wells can be very challenging as compression and buckling can be very high. The strong curve, local dog legs and long lateral section can increase significantly the level of compression and buckling along the string. It has been shown that standard buckling equations are not accurate enough to treat properly the problem, because of the complexity of the mathematical problem. These equations should be used cautiously and should be used as a guideline. A numerical model enabling to calculate the unknown contact points and the post-buckling behavior should be used to better quantify the severity of buckling for the planning and the operations.

A case study has been shown and highlight the importance of drilling quite smoothly the curve to not compromise the rest of the operation, as a lot of drag forces are produced in the curve, and possibly aggravated by local dog legs created by the steerable mud motor. Obviously drilling a smooth curve and lateral section in minimizing the tortuosity is key to avoid buckling.

Long lateral section drilled nowadays will require to use special techniques (floatation, rotation) to run completion at target depth. Accurate torque, drag, and buckling monitoring is key to avoid lock-up and failure and reach TD successfully.

Nomenclature

BHA = *Bottomhole assembly*
BSI = *Buckling Severity Index*
TFO = *Tool Face Orientation*
WOB = *Weight On Bit*

References

1. Lubinski A. : "A study On the Buckling Of Rotary Strings", API Drilling Production Practice, pp. 178-214, 1950.
2. Lubinsky A., Althouse W.S. and Logan J.L. : "Helical Buckling of Tubing Sealed in Packers", paper SPE 178, presented at the 36th Annual Fall Meeting of SPE, Oct. 8-11, Dallas, 1961
4. Dawson, R. and Paslay, P.R. 1984. Drill Pipe Buckling in Inclined Holes. J. Pet Tech 36 (10): 1734–1738.
5. Duman, O.B., Miska, S., and Kuru, E. 2003. Effect of Tool Joints on Contact Force and Axial-Force Transfer in Horizontal Wellbores. SPE Drill & Compl. 18 (3): 267–274.
6. Kyllingstad, A. 1995. Buckling of Tubular Strings in Curved Wells. J. Petrol. Sci. and Eng. 12: 209–218.
7. Lubinski, A. 1950. A Study of the Buckling of Rotary Strings. In API Drilling and Production Practice, 178–214.
8. Lubinski, A., Althouse, W.S., and Logan, J.L. 1961. Helical Buckling of Tubing Sealed in Packers. Paper SPE 178 presented at the 36th Annual Fall Meeting of SPE, Dallas, Texas, 8–11 October.
9. Mason, C.J. and Chen, D.C.K. 2007. Step Changes Needed to Modernize T&D Software. Paper SPE 104609 presented at the SPE/IADC Drilling Conference, Amsterdam, The Netherlands, 20–22 February.
10. Menand, S. 2012. A New Buckling Severity Index to Quantify Failure and Lock-up Risks in Highly Deviated Wells. Paper SPE 151279 presented at the SPE Deepwater Drilling and Completions Conference, Galveston, Texas, 20–21 June.
11. Menand, S., Bjorset, A., and Macresy, L. 2011. Tests Validate New Drill Pipe Buckling Model. Oil & Gas J. February.
12. Menand, S., Bjorset, A., and Macresy, L. 2011. A New Buckling Model Successfully Validated With Full-Scale Buckling Tests. Paper presented at the AADE 2011 National Technical Conference and Exhibition, Houston, Texas, 12–14 April.
13. Menand, S., Sellami, H., Akowanou, J. et al. 2008. How Drillstring Rotation Affects Critical Buckling Load? Paper SPE 112571 presented at the 2008 IADC/SPE Drilling Conference, Orlando, Florida, 4–6 March.
14. Menand, S., Sellami, H., Bouguecha, A. et al. 2009. Axial Force Transfer of Buckled Drill Pipe in Deviated Wells. Paper SPE 119861 presented at the 2009 IADC/SPE Drilling Conference, Amsterdam, The Netherlands, 17–19 March.
15. Menand, S., Sellami, H., Tijani, M. et al. 2006. Buckling of Tubulars in Actual Field Conditions. Paper SPE102850 presented at the 2006 SPE Annual Technical Conference and Exhibition, San Antonio, Texas, 24–27 September.
16. Mitchell, R.F. and Miska, S. 2004. Helical Buckling of Pipe With Connectors and Torque. Paper IADC/SPE 87205 presented at the IADC/SPE Drilling Conference, Dallas, Texas, 2–4 March.
17. Newman, K.R., Corrigan, M., and Cheatham, J.B. 1989. Safely Exceeding the Critical Buckling Load in Highly Deviated Holes. Paper SPE 19229 presented at the Offshore Europe 89, Aberdeen, 5–8 September.
18. Paslay, P.R. and Bogy, D.B. 1964. The Stability of a Circular Rod Laterally Constrained to Be in Contact With an Inclined Circular Cylinder. J. Appl. Mech. 31 (4): 605–610.

19. Schuh, F.J. 1991. The Critical Buckling Force and Stresses for Pipe in Inclined Curved Boreholes. Paper SPE/IADC 21942 presented at the 1991 SPE/IADC Drilling Conference, Amsterdam, The Netherlands, 11–14 March.
20. Tikhonov, V.S., Safronov, A.I., and Gelfat, M.Y. 2006. Method of Dynamic Analysis of Rod-in-Hole Buckling. Paper ESDA 2006-95059 presented at the ESDA 2006 8th Biennal ASME Conference on Engineering Systems Design and Analysis, Torino, Italy, 4–7 July.
21. Menand S., Chen D. "Safely Exceeding Buckling Loads in Long Horizontal Wells: Case Study in Shale Plays", paper SPE 163518, 2013 IADC/SPE Drilling Conference, Amsterdam, The Netherlands
22. Menand S., Mills K., Suarez R., "Micro Dogleg Detection with Continuous Inclination Measurements and Advanced BHA Modeling. SPE-183299-MS, ADIPEC 2016
22. Studer R., Simon S., Genevois J.M., Menand S. : "Learning Curve Benefits Resulting From the Use of a Unique BHA Directional Behaviour Drilling Performances Post-Analysis", paper SPE 110432, 2007 SPE Annual Technical Conference and Exhibition held in Anaheim, California, U.S.A., 11–14 November 2007

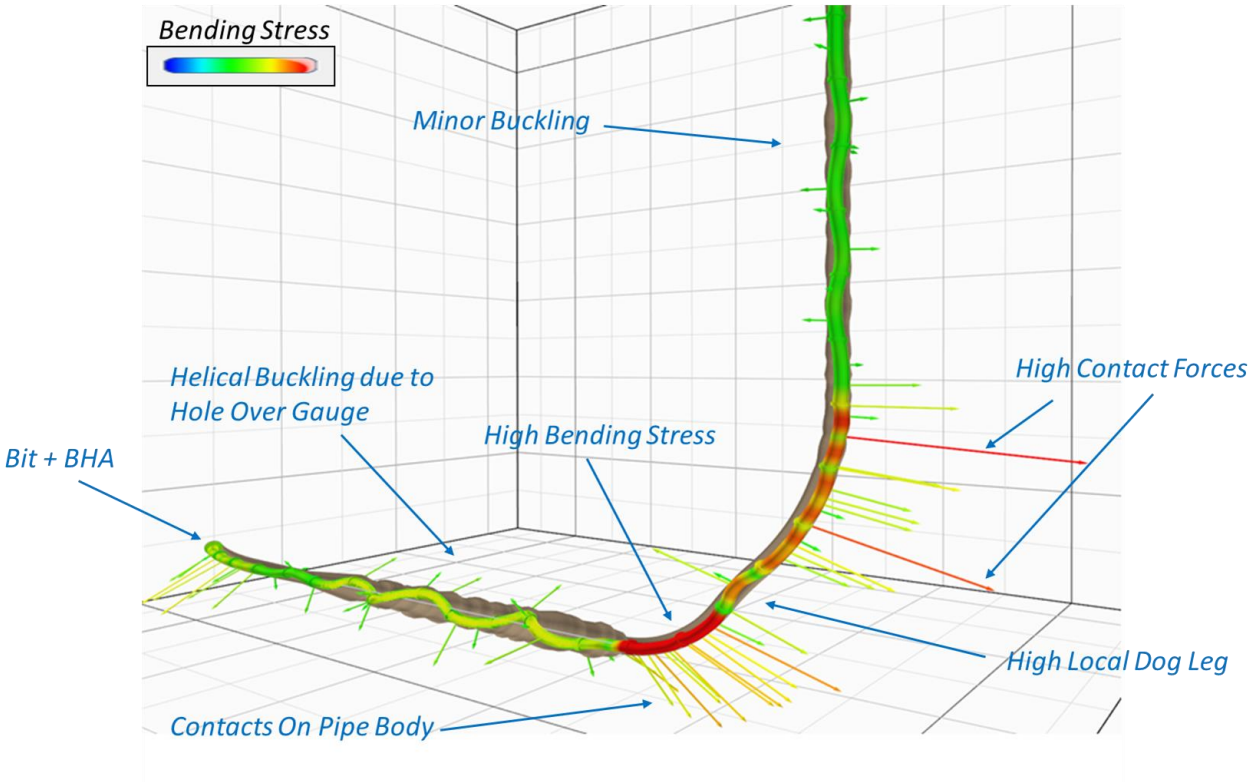

Figure 1: Typical buckling behavior in unconventional well – Bending Stress and Contact Forces (vectors)

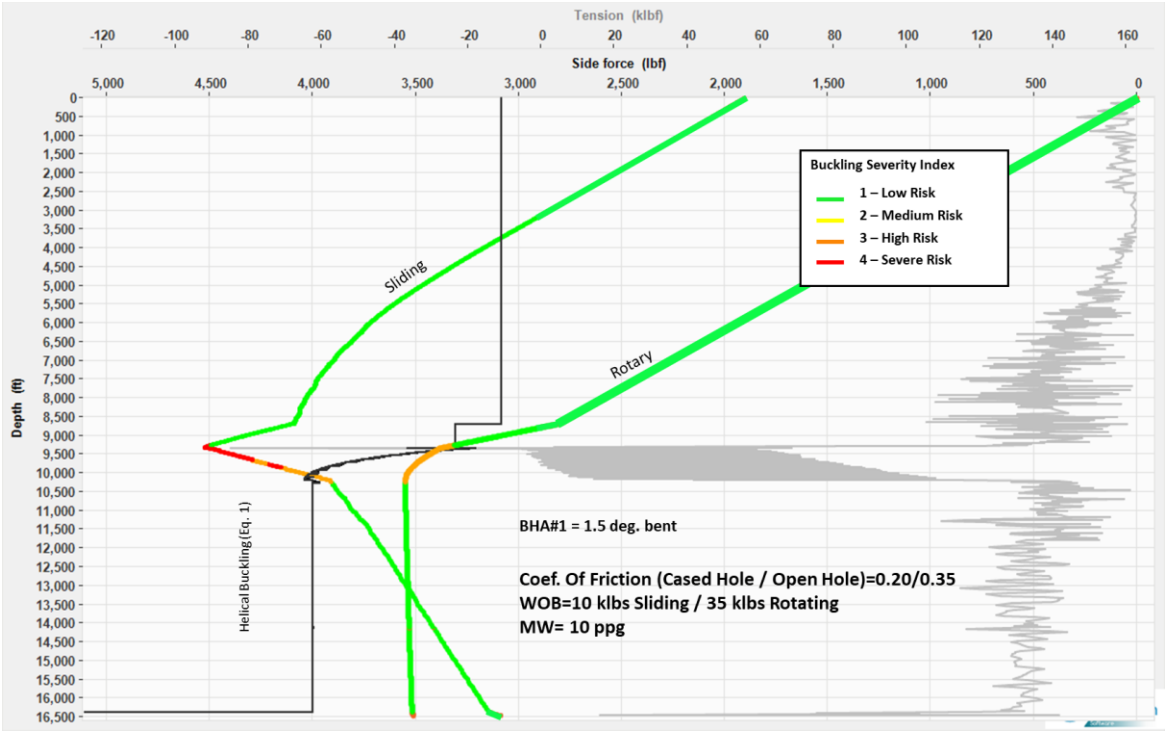

Figure 2: Tension/Compression, Side Force (sliding) along the drill string while drilling at target depth – Buckling Severity Index

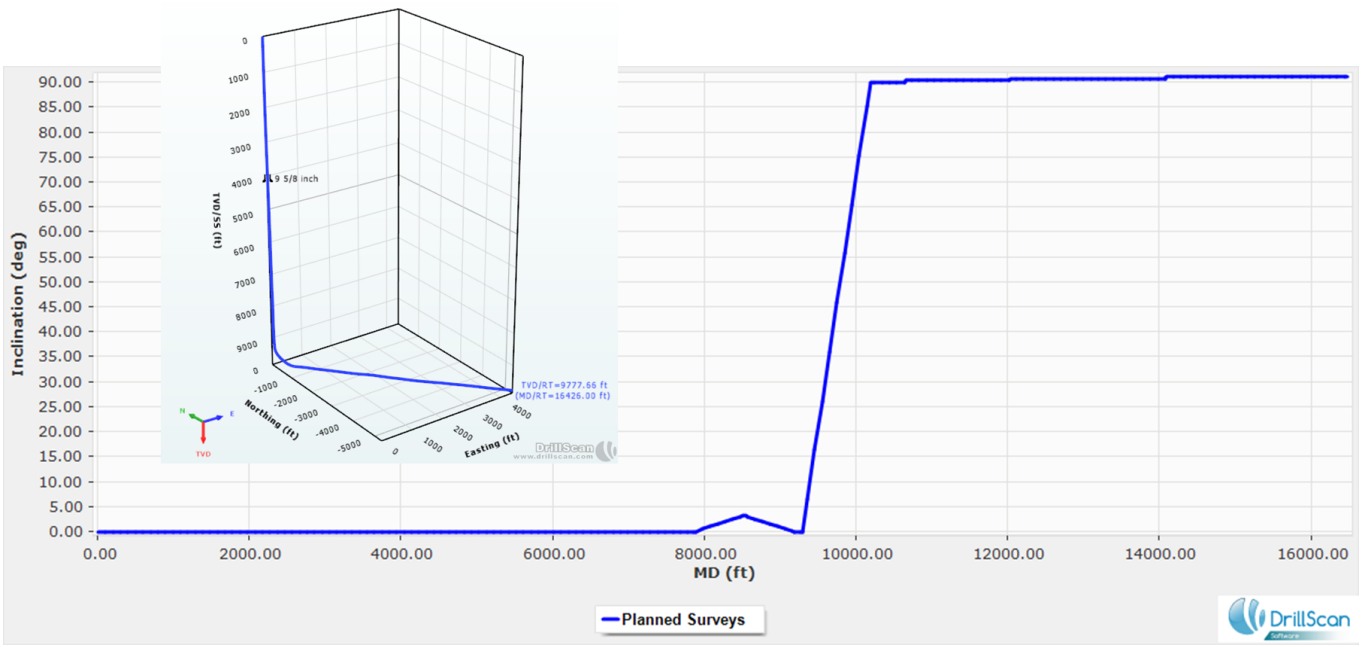

Figure 3: Well trajectory

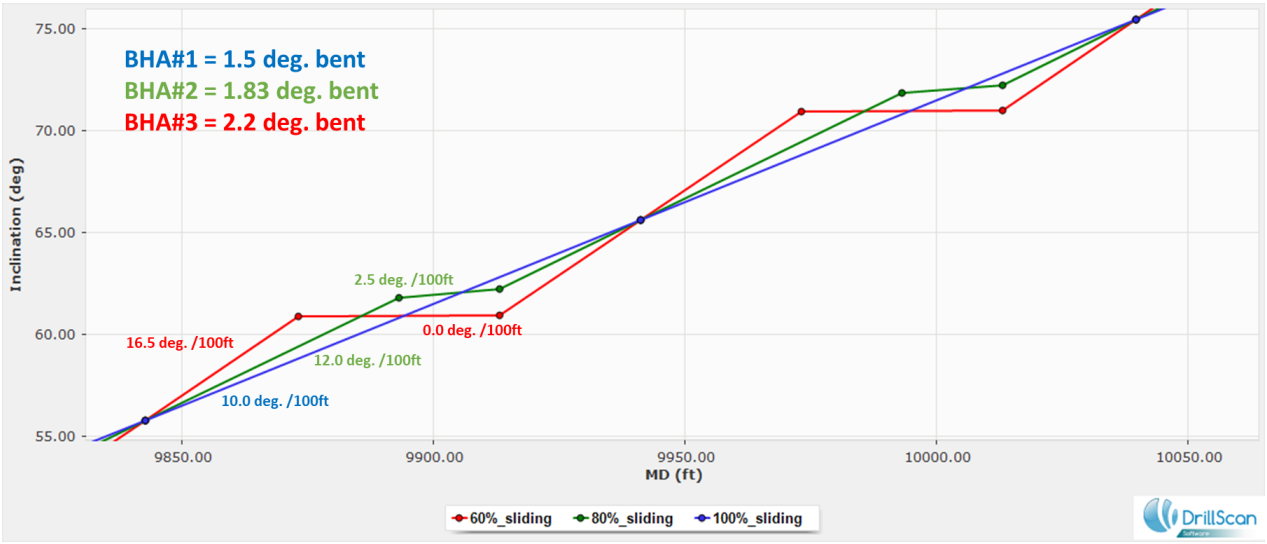

Figure 4: Three different slide-rotate patterns associated with 3 different BHAs (varying bend angle) along the curve

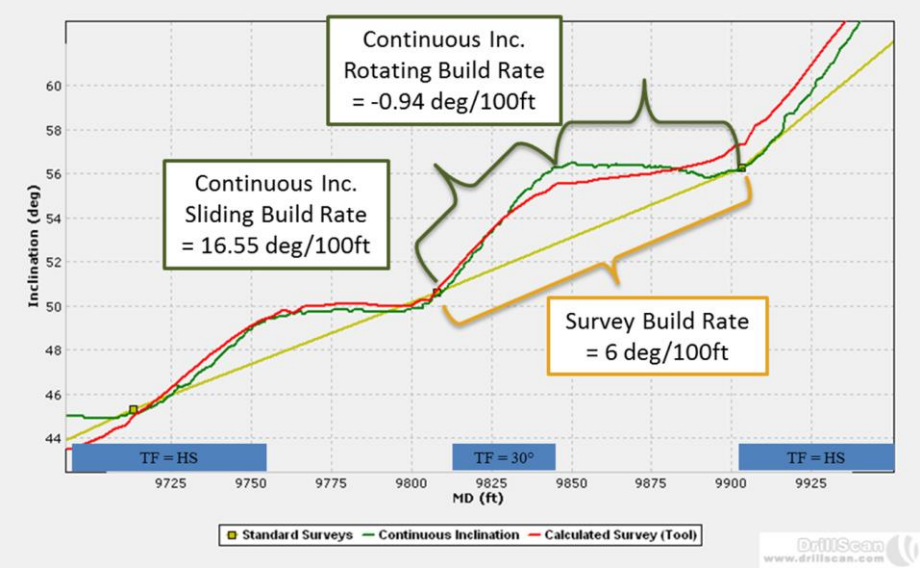

Figure 5: Typical Slide-Rotate pattern – source: SPE183299

Table 1: BHA characteristics

Type	Name	Length (ft)	OD (inch)	ID (inch)	Gauge (inch)	Total length (ft)	Contact (ft)	Mass (lb)	Total mass (lb)	Linear mass (lb/ft)
PDC	PDC L516	1.00	-	-	8 1/2	1.00	-	83.27	83.27	83.27
Steerable mud motor	5/6 4.5stg FBH 2 - 1.50	28.74	7	3	-	29.74	-	3072.74	3156.00	106.91
STA	-	-	-	-	7 1/8	-	3.50	-	-	-
BNT	-	-	-	-	-	-	5.00	-	-	-
Float sub x 1	Float sub	1.96	6 11/16	2 7/8	-	31.70	-	190.99	3346.99	97.44
DC x 1	Pony Collar	15.01	6 5/8	2 3/4	-	46.71	-	1457.47	4804.46	97.10
MWD	MWD	33.99	6 5/8	1	-	80.70	-	3896.64	8701.10	114.64
DC x 1	NMDC	29.50	6 1/2	2 7/8	-	110.20	-	2679.65	11380.75	90.84
DP x 75	19.5 X-95	2250.00	5	4.28	-	2360.20	-	48262.50	59643.25	21.45
Axial oscillation tool x 1	AOT	10.00	5	4.28	-	2370.20	-	178.59	59821.84	17.86
DP x 159	19.5 X-95	4770.00	5	4.28	-	7140.20	-	102316.50	162138.34	21.45
HWDP x 21		654.57	5	3	-	7794.77	-	38724.36	200862.70	59.16
DP x 1	19.5 X-95	30.00	5	4.28	-	7824.77	-	643.50	201506.20	21.45

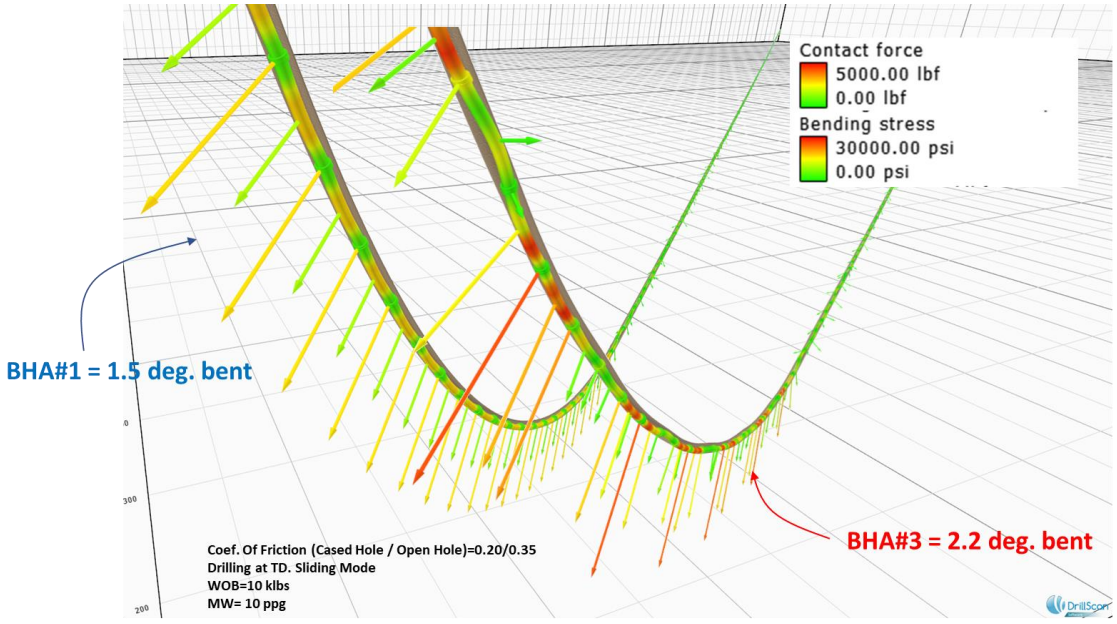

Figure 6: Bending stress and contact forces along the drill string along the curve

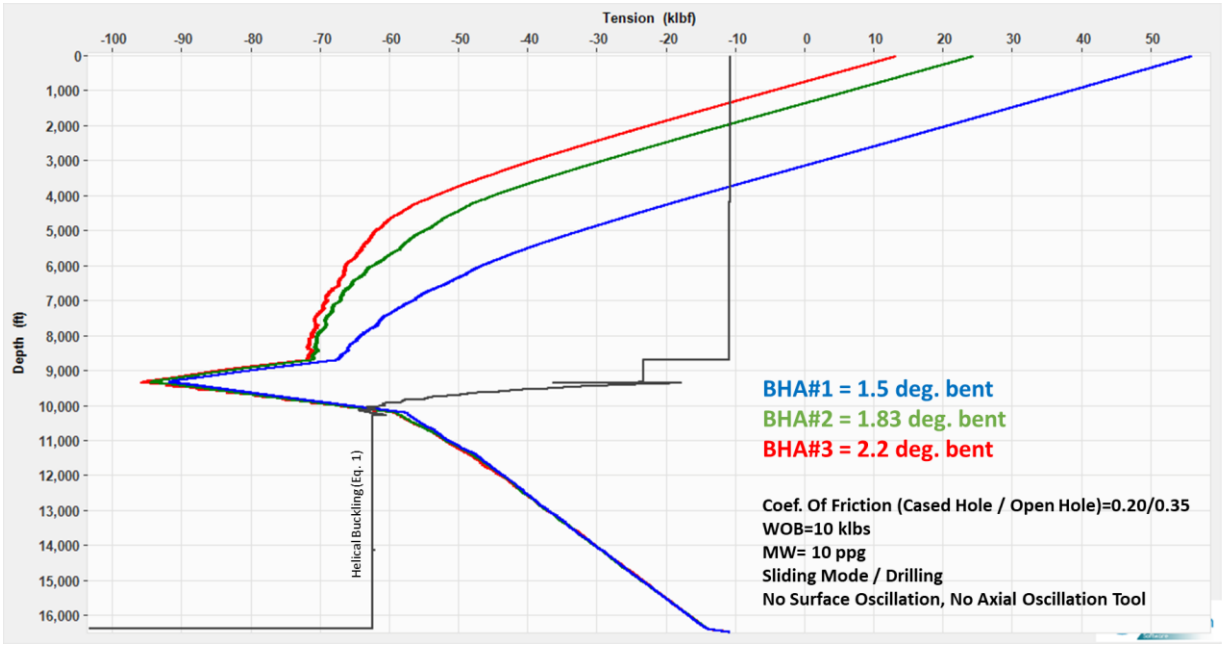

Figure 7: Tension/Compression along the drill string while drilling at target depth for the 3 BHAs

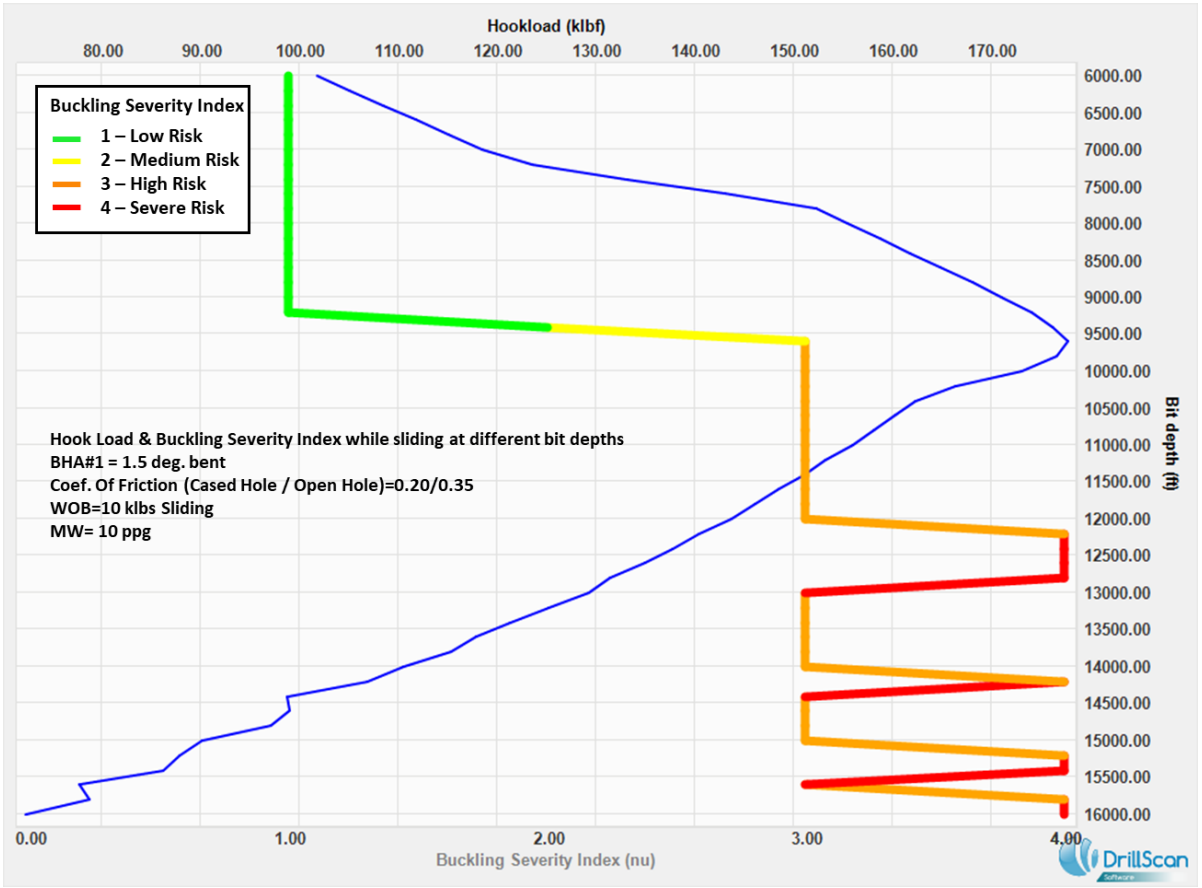

Figure 8: Hook Load & Buckling Severity Index while drilling in sliding mode

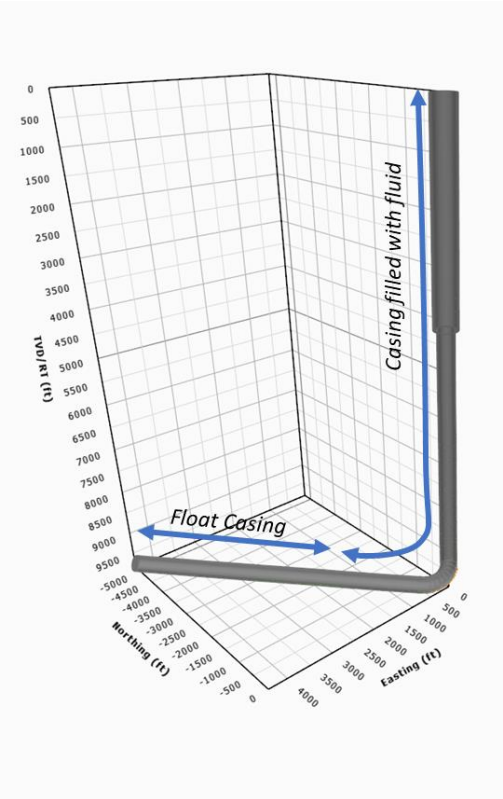

Figure 9: Basic schematics of the floated casing

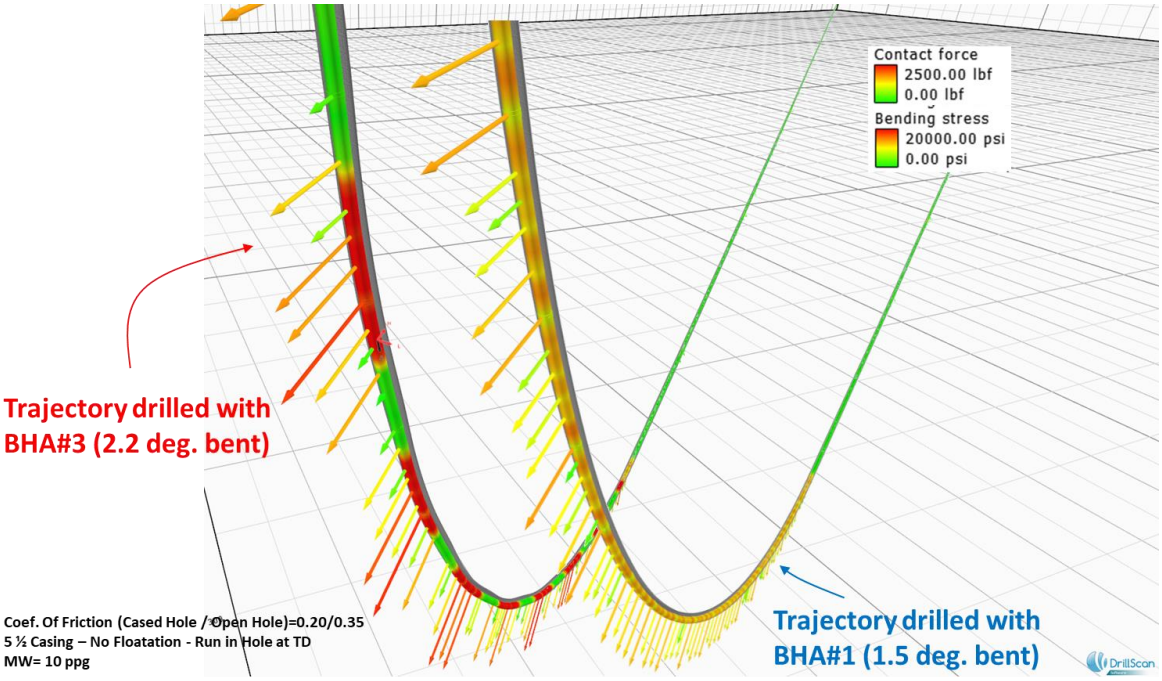

Figure 10: Bending stress and contact forces along the casing string along the curve while running in the hole at TD

Figure 11: Tension/Compression, Bending Stress along the casing string while running in hole at target depth

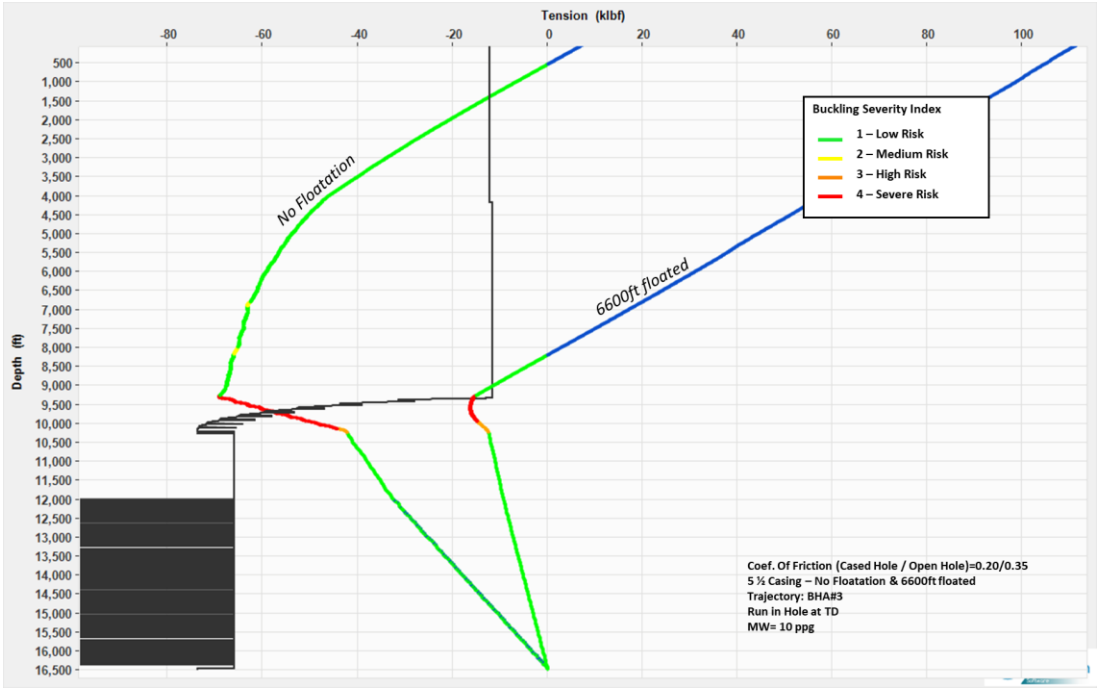

Figure 12: Tension/Compression, Buckling Severity Index along the casing string while running in hole at target depth

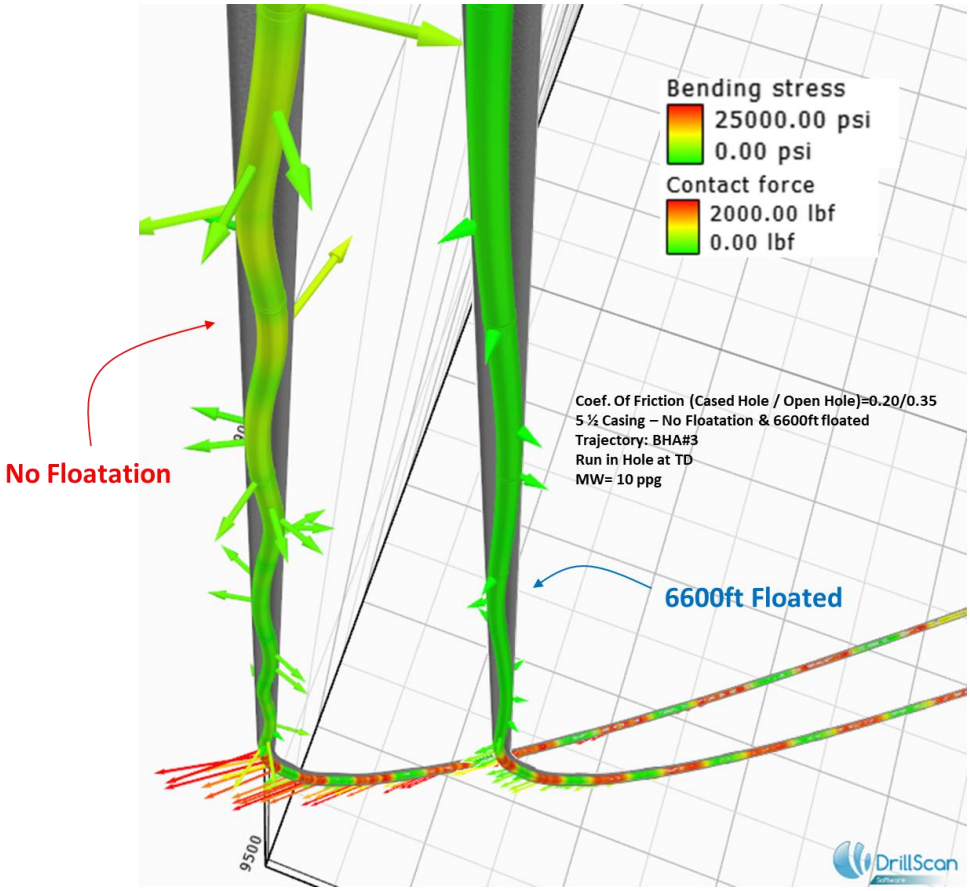

Figure 13: Bending stress and contact forces along the casing string while running in hole at target depth (vertical & curve sections)

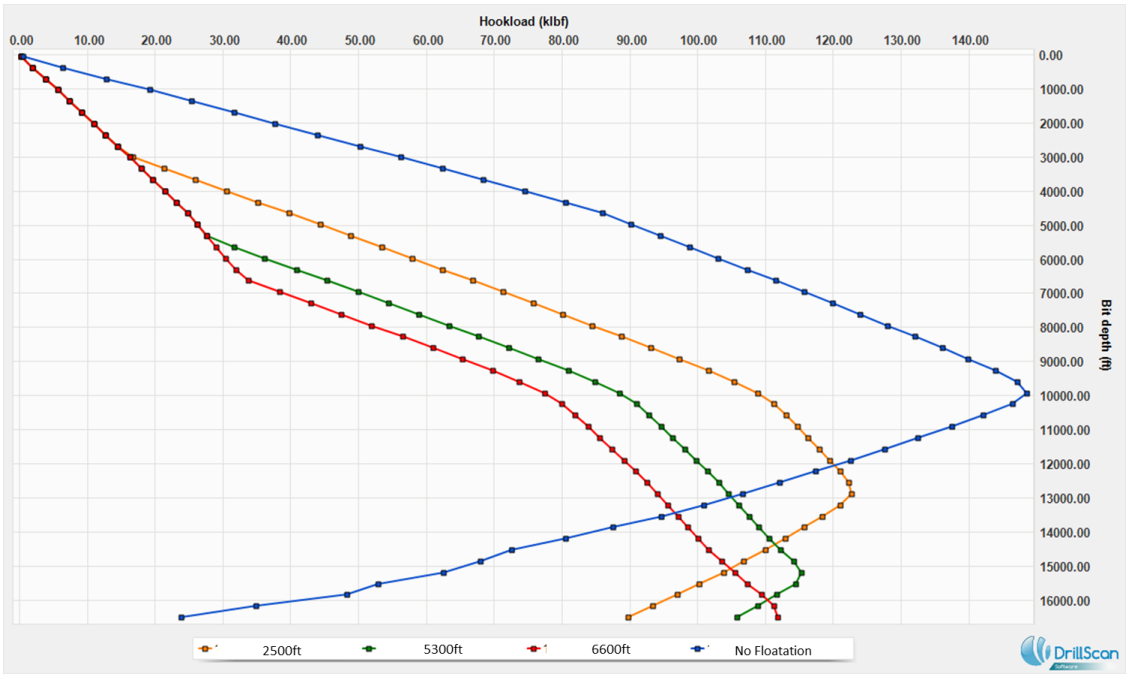

Figure 14: Hook Load while running in hole the casing string. No floatation, 2500ft, 5300ft and 6600ft floated casing. Coefficient of friction = 0.20/0.35 (Cased Hole/ Open Hole)